



Supplement of

Mercury oxidation from bromine chemistry in the free troposphere over the southeastern US

S. Coburn et al.

Correspondence to: R. Volkamer (rainer.volkamer@colorado.edu)

The copyright of individual parts of the supplement might differ from the CC-BY 3.0 licence.

24 **Instrument and Measurement Site**

25 The instrument and measurement site are identical to that described in Coburn et al. (2011). Only
26 a brief overview will be given here. For the duration of the measurements discussed in this study,
27 a research-grade MAX-DOAS instrument was located at a United States Environmental Protection
28 Agency (US EPA) facility in Gulf Breeze, FL (30.3N 87.2W) and measured for time periods between
29 May 2009 and February 2011. This site is ~10 km southeast of Pensacola, FL (population appr.
30 50,000) and ~1 km from the coast of the Gulf of Mexico, which enables the measurement of
31 urban and marine air masses. The spectrometer and controlling electronics were set-up in the
32 warehouse of the EPA facility, while the telescope was mounted on a support structure on the
33 roof of the warehouse (~10-12 m above sea level) connected via an optical fiber. The telescope
34 was oriented ~40° west of true north in order to realize a clear view in the lowest elevation angles
35 to the coast. During operation the full 180° elevation angle range of the telescope was utilized to
36 enable the characterization of air-masses over the seawater lagoon to the North, and over the
37 coastal region of the Gulf of Mexico to the South. For the purposes of this study, the north viewing
38 direction will be considered to minimize changes in the radiative transfer calculations due to
39 azimuth effects throughout the day.

40 The instrument used for this study consists of a Princeton Instruments Acton SP2300i Czerny-
41 Turner grating (500 groove/mm with a 300nm blaze angle) spectrometer with a PIXIS 400B back-
42 illuminated CCD detector (Coburn et al., 2011). This setup was optimized to cover the wavelength
43 range ~321-488 nm with an optical resolution of ~0.68 nm full-width at half the maximum
44 (FWHM). The spectrometer is coupled to a weather-resistant telescope (capable of rotating the
45 elevation angle by 180°, 50 mm f/4 optics) via a 10 m long 1.7 mm diameter quartz fiber. During
46 normal field operation this instrument was routinely able to realize values of the root mean
47 square (RMS) of the residual remaining after the DOAS fitting procedure on the order $0.9-3 \times 10^{-4}$.
48 This system was very stable, with little need for maintenance, and was operated remotely for
49 periods between May 2009 and February 2011 to measure multiple trace gases, including: BrO,
50 IO, nitrogen dioxide (NO₂), formaldehyde (HCHO), glyoxal (CHOCHO), and the oxygen molecule
51 collision induced absorption signal (referred to as O₄).

52 **Aerosol Retrieval**

53 Aerosol profiles are determined through an iterative comparison of measured O₄ dSCDs
54 (analyzed in the wavelength window 437-486 nm) with O₄ dSCDs calculated from the RTM
55 McArtim3 (Deutschmann et al., 2011) outputs based on specific aerosol extinction profiles. This
56 process is performed on each set of MAX-DOAS viewing angles (for this point forward referred
57 to as a scan) of the case study day (total of 56 scans) in order to determine individual aerosol
58 profiles. The initial aerosol profile used for each scan decreased exponentially with altitude from
59 a value of 0.01 km⁻¹ at 483 nm (scale height of 0.6 km). This wavelength is chosen for its proximity
60 to the O₄ peak absorption structure at 477 nm while avoiding the feature itself, as well as avoiding
61 absorption structures from other trace gases (i.e. NO₂).

62 The O₄ vertical profiles used for all calculations and as input to the RTM are based on temperature
63 and pressure profiles available from NOAA's ESRL Radiosonde Database for locations close to the
64 measurement site, which are in good agreement with the corresponding profiles from WACCM.
65 In each step of the iteration the measured O₄ dSCDs are compared to the forward calculated
66 dSCDs at each elevation angle of the scan being analyzed, and the differences between these
67 values are used as input for optimizing the modification of the aerosol profile for the subsequent
68 iteration. For this study, the convergence limit is set at a percent difference of 5% between the
69 lowest two elevation angle dSCDs, or if the process reaches 5 iterations without finding
70 convergence the last aerosol profile is used. The limit of 5 iterations is chosen as a compromise
71 between achieving optimal agreement between the O₄ dSCDs and data computation time. For
72 this case study, the 5% criterion is reached for every sequence. The resulting time series of
73 aerosol extinction profiles are shown in Fig. S8 (Supplement).

74 The aerosol extinction profiles at 483 nm were scaled to derive extinction at 350 nm using the
75 relationship found in Eq. (S1).

$$76 \quad \epsilon_{350} = \epsilon_{483} \cdot \left(\frac{350}{483}\right)^{-1.25} \quad (S1)$$

77 where ϵ_{350} and ϵ_{483} represent aerosol extinction coefficients at 350 and 483 nm, respectively. The
78 retrieved aerosol profiles at 350 nm provided input to the RTM in order to calculate the
79 appropriate weighting functions for BrO.

80 **Box Model Description**

81 The modeling portion of this study is designed to assess the concentration of Br radicals available
82 to participate in the mercury oxidation reaction based on BrO vertical profiles provided from the
83 MAX-DOAS measurements and the WACCM CTM. Inputs to the diurnal steady-state box model
84 (Dix et al., 2013, Wang et al., 2015) are median daily profiles derived from the MAX-DOAS
85 measurements and/or the WACCM CTM. A single median profile representing the entire day
86 (daily median, for each model input) is used rather than individual profiles. From these profiles,
87 the box model then calculates the partitioning between bromine species throughout the
88 troposphere (including: reactions with other trace gases; photolysis; and some aqueous phase
89 partitioning and chemistry) in order to derive vertical profiles of the Br radical, which are
90 subsequently used for calculating mercury oxidation rates. A summary of all the reactions
91 involving mercury compounds considered in the box model along with associated rate
92 coefficients can be found in Table 2. The model conceptually follows the framework of Crawford
93 et al., (1999), where model inputs are initiated and allowed to reach steady-state over several
94 days. In the box model, the BrO and IO (to assess the impact of iodine radical species in the
95 mercury oxidation reactions) profiles are taken from the MAX-DOAS measurements; however,
96 WACCM and GEOS-Chem BrO profiles are also used in order to assess the impact of the
97 differences between these profiles. Other model inputs are taken as the output profiles from
98 WACCM for the case study day, and these included: temperature, pressure, O₃, HCHO, and NO₂.
99 Aerosol surface area measurements and GEM estimates from the TORERO data set (Volkamer et
100 al., 2015; Wang et al., 2015) are assumed representative of conditions in the marine atmosphere,
101 and therefore used as model inputs for lack of independent measurements. Additionally,
102 photolysis rates for a variety of species, calculated using the Tropospheric Ultraviolet and Visible
103 (TUV) Radiation model, are included. The TUV model was initiated for a Rayleigh atmosphere
104 (aerosol extinction = 0), with O₃ and NO₂ columns of 380 and 0.3 Dobson Units (DU), respectively,
105 which are derived from the average vertical profiles from WACCM. Since the median BrO profile
106 derived by the MAX-DOAS measurements closely resembles the profiles retrieved around solar
107 noon (see Fig. 5), the TUV calculations from this time are used. For the model runs comparing the
108 BrO profiles from the measurements, WACCM, and GEOS-Chem, only the BrO profile is changed;
109 all other inputs remain constant.

110 For the determination of the dominant oxidative pathways, the reaction rates for oxidation of
111 Hg^0 against Br, O_3 , and Cl are calculated as a function of altitude for the different reactant vertical
112 profiles, which is important due to atmospheric temperature gradients. This also allows the
113 assessment of the relative contributions of these reactions to the overall rate of oxidation as a
114 function of altitude. Oxidation by O_3 is included in the box model due to the amount of evidence
115 from laboratory studies indicating that this reaction might play a role in the atmosphere;
116 although potentially not completely in the gas phase. The reaction between GEM and Cl is
117 expected to proceed via a mechanism similar to that between GEM and Br and has been found
118 to be quite fast (Donohoue et al., 2005), as well as energetically favorable (Tossell 2003). For
119 these reasons it is also included in the box model.

120 Following Wang et al. (2015), the box model is initiated under two different modes to investigate
121 the sensitivity of oxidation rates, and likely product distributions to the mechanistic assumptions
122 about mercury oxidation. The two modes differ in the scavenging reactions of the HgBr adduct.
123 A “traditional” scenario only includes Br and OH radicals as scavengers (Holmes et al., 2009), and
124 a “revised” mode includes species suggested by Dibble et al., 2012 (BrO, NO_2 , and HO_2) as well
125 as additional halogen species (I and IO). The model also tracks the concentrations of all species
126 as a function of altitude, which gives indications for the product distributions of the various
127 reactions.

128

129 **Figure Captions**

130 **Figure S1:** BrO box-AMFs for two elevation angles (25° and 90°, solid and dashed lines
131 respectively) at different SZAs. For these higher pointing elevation angles, the box-AMFs peak at
132 altitudes of 2-15km (free troposphere) for SZAs lower than 70°, while at higher SZA the box-AMFs
133 indicate that the sensitivity towards the free troposphere is decreasing.

134 **Figure S2:** Overview of box-AMFs for SZAs less than 70° for 4 elevation angles: a) 3.8°; b) 10°; c)
135 25°; and d) 90°.

136 **Figure S3:** Overview of the WACCM BrO vertical profiles as a function of altitude and time of day
137 (panel a), and then collapsed into to the corresponding partial (green trace) and total (blue trace)
138 VCDs in panel b.

139 **Figure S4:** Example results for the inversion of IO from the MAX-DOAS measurements. Panel a)
140 contains the three a-priori profiles used in the inversion (dashed, colored lines), the a-posteriori
141 results from a MAX-DOAS scan at ~45° SZA (morning) corresponding to the a-priori profiles (solid
142 lines, colors correspond with the a-priori), and the median IO profile (red trace, where the error
143 bars reflect the 25th and 75th percentiles). Panel b) shows the averaging kernels for the inversion
144 using a-priori “Prf1”. Panel c) shows the diurnal variation of the IO VCD for the BL (0-1 km),
145 troposphere (0-15 km), and total (0-25 km).

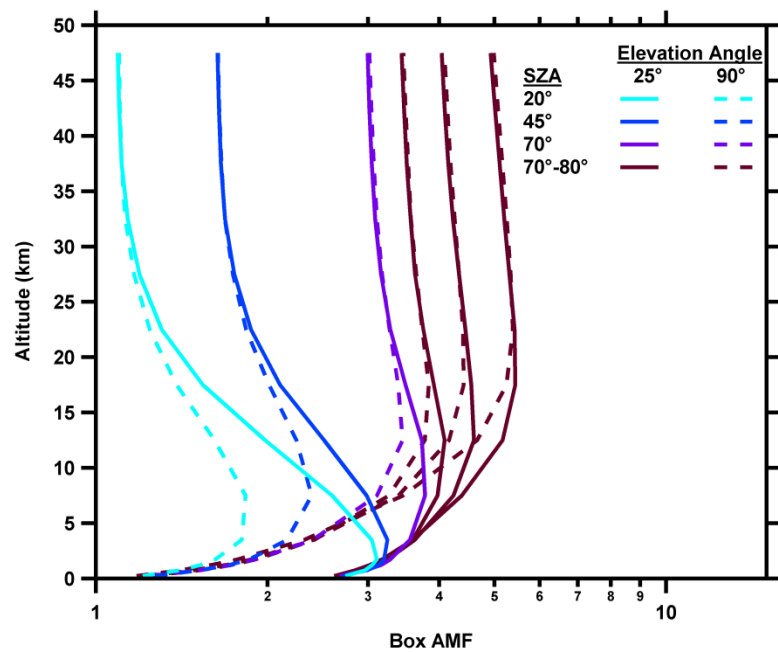
146 **Figure S5:** Overview of the sensitivity of SCD_{Ref} and the derived VCDs on the choice of reference
147 spectra/scan and a-priori profile assumption. Panel (a) contains the SCD_{Ref} determined from both
148 forward calculations of the a-priori profiles (grey traces) and the iterative approach (blue traces)
149 for 47 different zenith spectra. The a-priori cases corresponding to the median BrO profile based
150 on WACCM (WACCM*1.4) are denoted with thicker and darker lines. The error bars on the
151 forward calculated median BrO profile case (dark grey) reflect the $\pm 1 \times 10^{13}$ molec cm⁻² criteria for
152 selecting suitable references. Panel (b) contains the corresponding VCDs derived for one MAX-
153 DOAS scan (near solar noon) for each of the references and a-priori combinations. The blue
154 shaded vertical boxes denote references that meet the criteria for being used in the inversion;
155 and the horizontal grey box (panel b) covers the range of $2.3 \pm 0.9 \times 10^{13}$ molec cm⁻², which fully
156 captures all the references contained within the shaded blue region.

157 **Figure S6:** Time series of the DoFs and inversion RMS for three different analysis procedures: 1)
158 changing reference analysis (reference is selected from each measurement scan throughout the
159 day, blue trace); 2) fixed reference without accounting for any SCD_{Ref} (green trace); and 3) fixed
160 reference analysis accounting for SCD_{Ref} (red trace). Included in the plot is SZA (black trace) for
161 reference.

162 **Figure S7:** Shows a comparison of the measured BrO dSCDs and the dSCDs calculated from the a-
163 posteriori profiles (inversion using the WACCM profile) for both the entire case study day (panel
164 a) and for a small subset of scans before solar noon (panel b). Panel c contains the RMS of the
165 difference between the measured and calculated dSCDs for each scan.

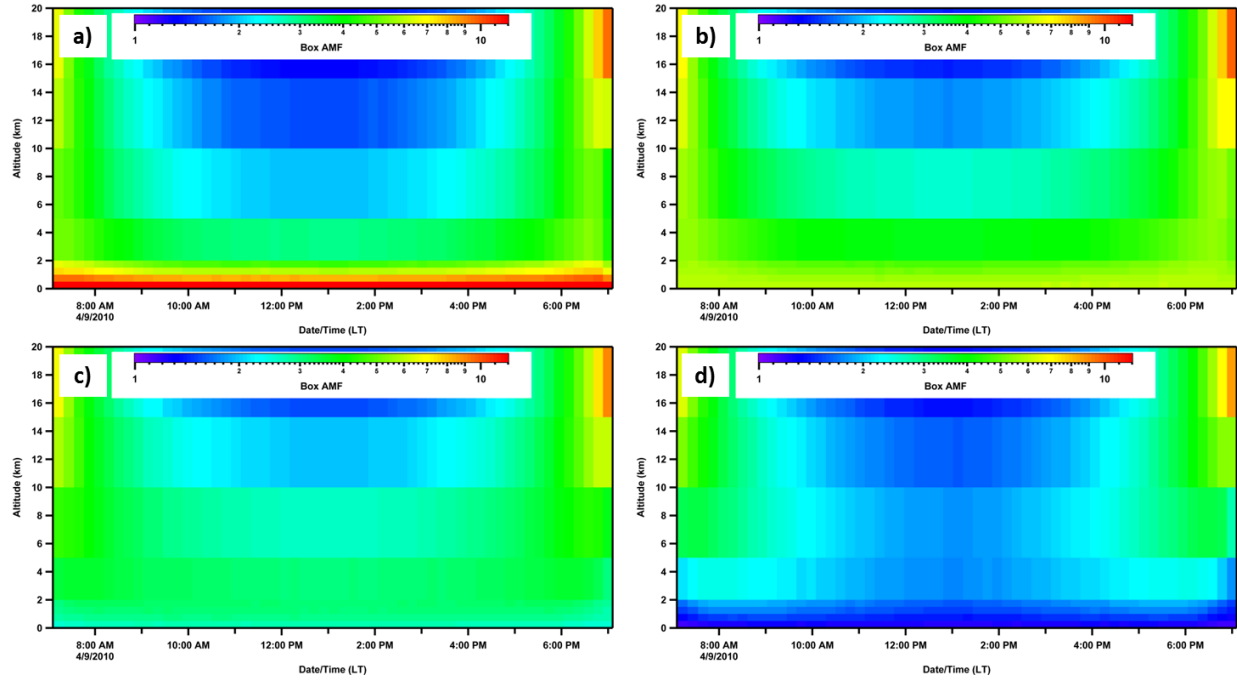
166 **Figure S8:** Observed concentrations of selected trace gases during April 2010 at the Pensacola
167 MDN site. Note scale factors for some species given in the legend.

168 **Figure S9:** Comparison of measured O_4 dSCDs and dSCD calculated based on the derived
169 aerosol profiles for the entire case study day (panel a) and a subset of scans (panel b). Panel c
170 contains the diurnal variation in the derived aerosol profiles, and an example profile is found in
171 panel d.



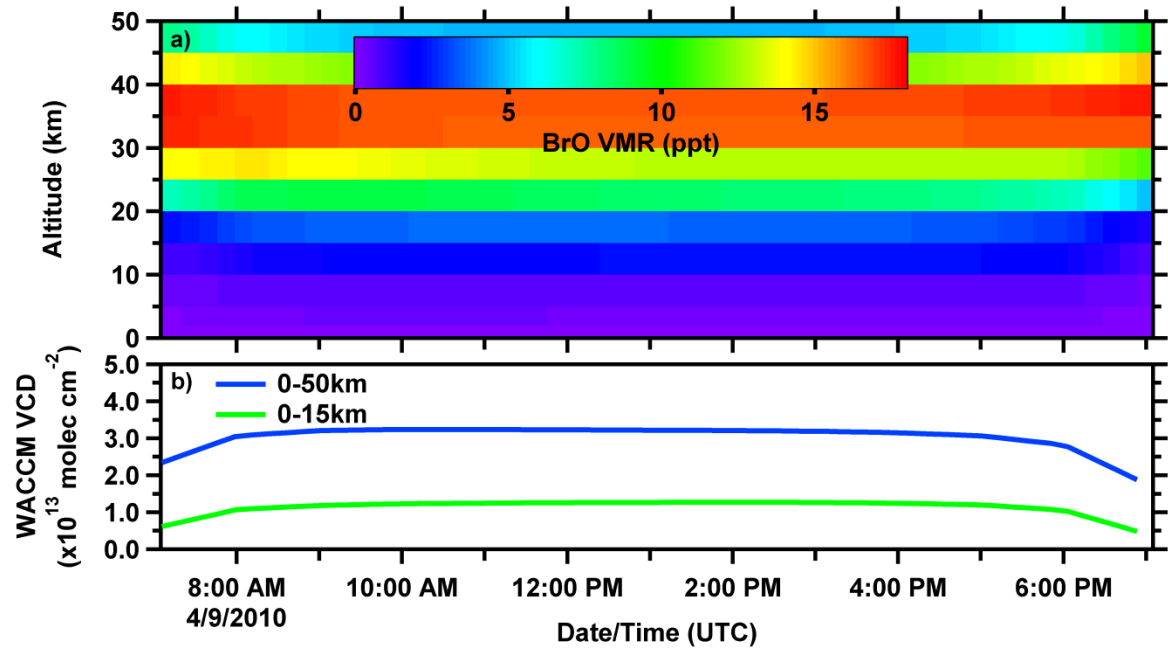
172

173 Figure S1



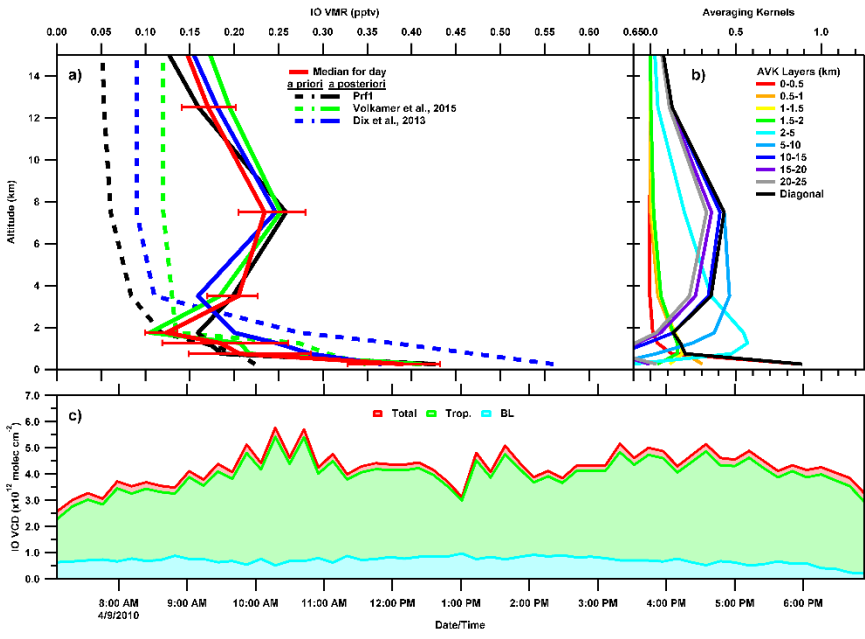
174

175 Figure S2



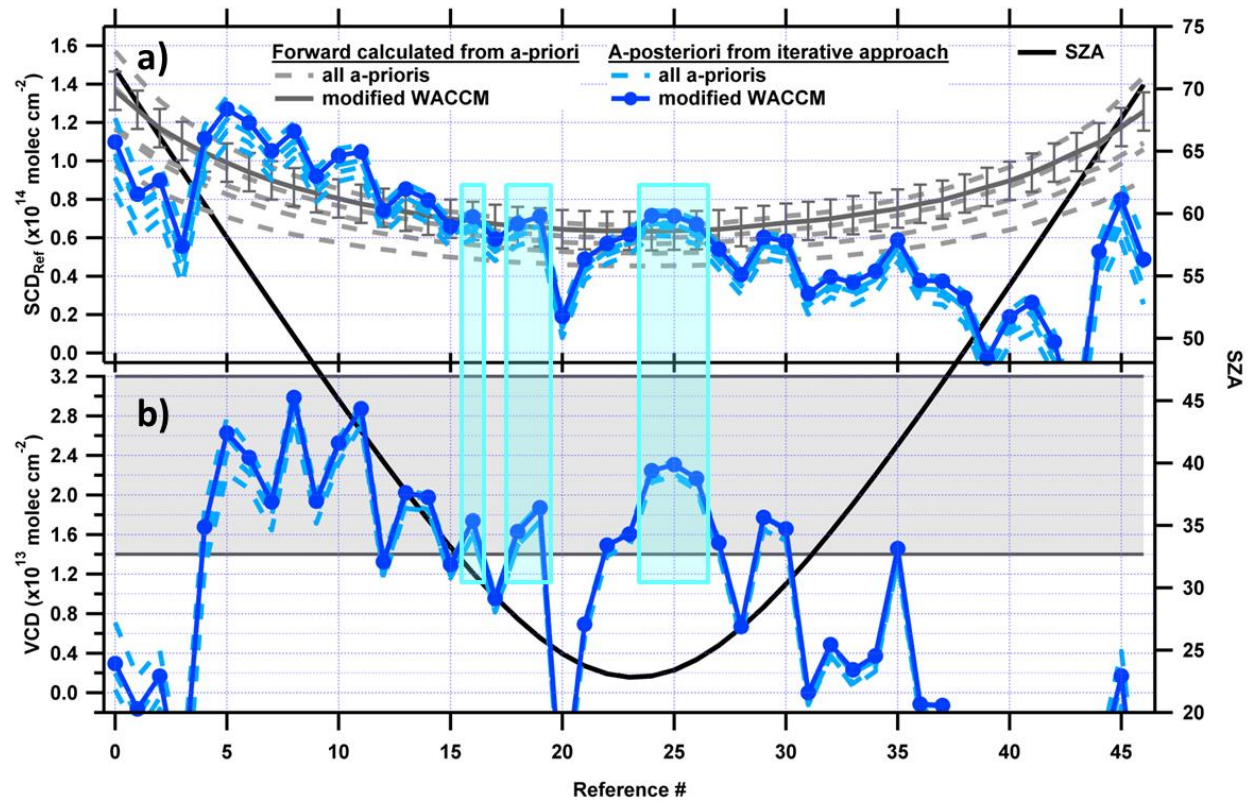
176

177 Figure S3



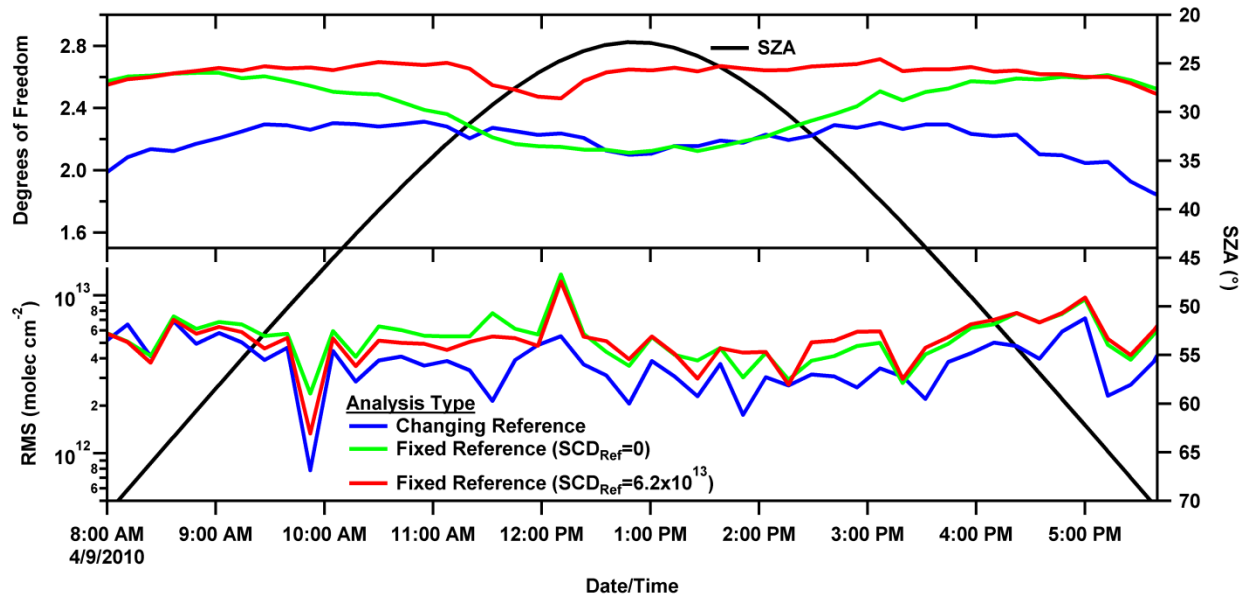
178

179 Figure S4



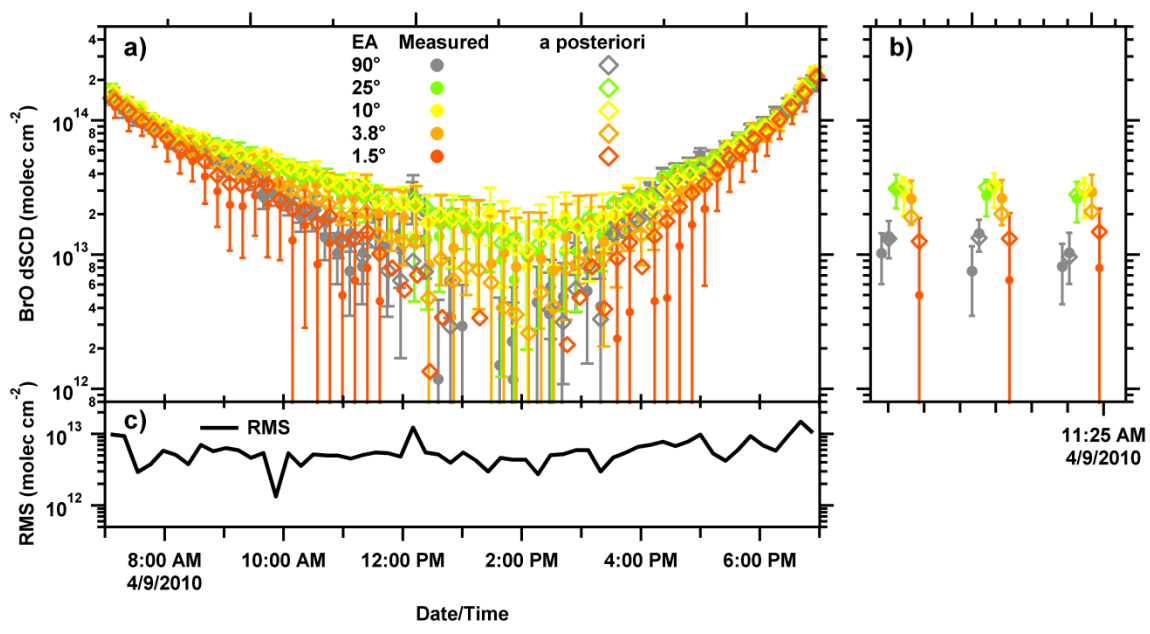
180

181 Figure S5



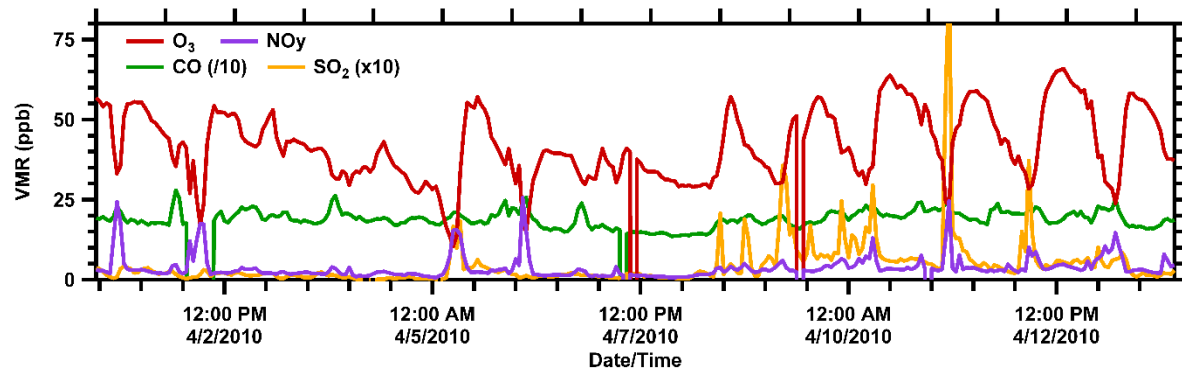
182

183 Figure S6



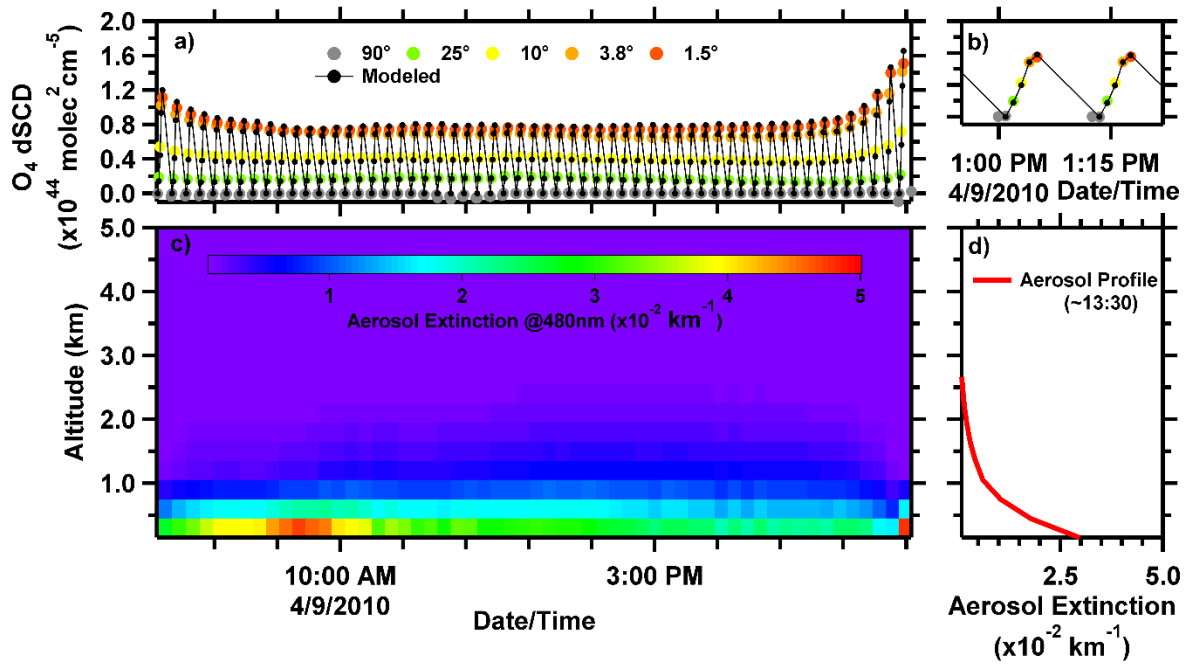
184

185 Figure S7



186

187 Figure S8



188

189 Figure S9